Determination of the behavior and performance of commercial Li-Ion pouch cells by means of isothermal calorimeter

Khan, Mohammad Rezwan; Swierczynski, Maciej Jozef; Kær, Søren Knudsen

Published in:
Proceedings of 2016 Eleventh International Conference on Ecological Vehicles and Renewable Energies (EVER)

DOI (link to publication from Publisher):
10.1109/EVER.2016.7476441

Publication date:
2016

Document Version
Early version, also known as pre-print

2016 Eleventh International Conference on Ecological Vehicles and Renewable Energies (EVER)

Determination of the Behavior and Performance of Commercial Li-Ion Pouch Cells by Means of Isothermal Calorimeter

Mohammad Rezwan Khan, Maciej Jozef Swierczynski, Søren Knudsen Kær
Department of Energy Technology, Pontoppidanstræde 101, Aalborg University, DK-9220 Aalborg, Denmark
Email: rezwankhn@gmail.com;mrk@et.aau.dk

Abstract— **In this experiment-based research, there is an attempt to determine the evolution of surface temperature distribution, thermal behaviour and performance of a battery cell at the same time. The pouch type commercial test cell has a 13Ah capacity and Lithium Titanate Oxide (LTO) based anode. Temperatures on the surface of the cell are measured using contact thermocouples. Additionally, the heat flux is simultaneously measured with the isothermal calorimeter. This heat flux measurement is used for determining the heat generation inside the cell. Consequently, the important performance constituent of the battery cell efficiency is calculated. Those are accomplished at different temperature levels (0°C and 25°C) of continuous constant current 1C charge and discharge. Also, the maximal increase in the battery temperature over the cell surface is found on the battery cell surface. The heat flow calibration and experimentation for calorimetric measurement are deliberated. The experimental procedure is a very precise determination of the heat generation and the efficiency of the battery cell.**

Keywords— Surface temperature, spatial tempersture distribution, Isothermal Calorimeter, Lithium Titanate Oxide, Battery thermal management, battery efficiency, heat generation, performance, battery behavior.

I. INTRODUCTION

In different operating conditions, the non-uniformity of the surface temperature is a result of the possible heat generation inside a battery cell [1, 2]. This is true for different battery applications, from stationary storage to the electric vehicle (EV) application [3, 4]. From the electrochemical point of view, this stems from complex phenomena inside the cell [5-7]. It is demonstrated in the literature how different operating conditions (e.g., unbalanced state of charge (SoC) [8, 9], different aging conditions [10, 11], flow rates [12-14] non-exhausting list of parameters) may affect battery cells' performance and can cause thermal gradients. Moreover, it is found that there is a correlation between heat generation and the maximal increase of temperature inside the cell [15]. So, it is essential to understand those behaviors and performance indicators. It can help to understand the individual cell behavior inside a pack [16]. Moreover, it makes possible to assure the correct operation of the battery cell on the system level.

Furthermore, another important parameter, battery cell efficiency, can assist in an optimized design of battery thermal management system (BTMS) [7, 17, 18]. This is particularly true in the case of battery system design. One aspect of the problem is that there is usually a little or no knowledge about the exact composition of the actual battery cell. The battery cell is made up of non-homogeneous materials. So it may exhibit different heating behavior on the battery cell surface [19]. In consequence, thermal modeling becomes more challenging as well as designing of efficient thermal management for battery system for different applications. Another limiting factor is the finite number of temperature sensors that can be mounted due to cost and practical reason. For a given current rate, it is crucial to understand the phenomenon of the surface temperature evolution with the heat produced inside the cell. So, a thermal model can be developed later. This can assist in the efficient cooling of the location of the hottest region on the battery surface.

In the paper, Section II presents the methodology that is used in this study. The detailed experimental procedures with necessary apparatuses i.e. thermocouples, calorimeter, and temperature controller are described in Section III. It also associates the data acquisition platform, calibration of the corresponding instrument and the final setup of the experiment. The analysis of the data and the relevant discussions are detailed in Section IV. The

evaluation of the cell thermal behavior and the experimental correlation is addressed and established in the same section. At last, the conclusions of this work are provided in Section V.

II. Methodology

The research associates with the determination of heat generation and efficiency of a battery cell using full charge and discharge cycle at different temperatures using experimental recourse. During the experiment, the principal thermal features of the battery cell are measured. Those are battery cell raw heat flux (measured using isothermal calorimeter) and surface temperature (measured using contact thermocouples) at different spots. Those are simultaneously measured to track the thermal gradients on the surface of the battery. Calorimetric measurement represents the global heat generation flux inside the cell at the given current profile. By using this calorimetric raw heat flux data, the battery heat generation is determined. To accomplish this, a suitable range of raw heat flux is carefully chosen. The next procedure is to select the best baseline type to find the enclosed heat flux area. Then by means of the use of computational software, the actual heat generation is determined. Afterward, using the electrical (area enclosed by electric power input) and calorimetric data (area enclosed by heat flux), the efficiency of the battery cell is calculated at the corresponding current rate. Congruently, the maximal increase in the battery temperature inside cell surface is found for different current rates on the battery cell surface.

III. Experimental Procedure

Battery thermal measurements in this research are accomplished by contact thermocouples in the calorimeter chamber with temperature control. The experimental setup is controlled by graphical user interface (GUI) of LabVIEW front panel interface. Fig. 1 illustrates the graphical representation of the experimental setup.

A. Thermocouple

The battery cell temperature measurement system is made of five type K thermocouples. The five thermocouples are manufactured by Netzsch® from raw 30 American wire gauge (AWG) wires. Those are situated inside the calorimeter chamber. By this way, those can be placed on the battery cell sample itself to measure the temperature distribution over the surface without disturbing the experimental condition. The specific connections inside the battery cell are shown in Fig. 6. The module used for the data acquisition of temperature measurements is a 4-channel module 9211 from the National Instruments®.

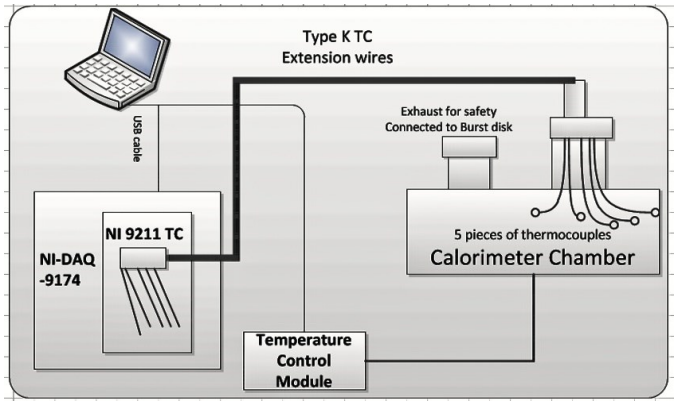

Fig. 1. The thermal sensor and control components inside the calorimeter. It consists of three parts: thermocouples, calorimeter, temperature control.

B. IBC 284 Calorimeter

The Isothermal Battery Calorimeter Netzsch® IBC 284 is a robust instrument designed for the accurate measurement of heat flux generated by batteries while being charged or discharged under experimental condition. This large volume calorimeter is made up of different thermal chambers and heat flux sensors submerged in an isothermal bath comprising a heating element, a cooling element, and a mixing system. It has an operating span of -30°C to +60°C. A mixture of 50% ethylene glycol and 50% deionized water (EG/W) is used to ensure the isothermal environment inside the bath. The following TABLE I. exhibits the specification of the calorimeter.

TABLE I. The IBC 284 calorimeter specification.

Temperature range	-30°C to +60°C
Isothermal bath stability	±0.01°C
Heating / Cooling rate	5°C / hour
Sample thermocouples available	4
Refrigerated recirculator	Built-in to unit
Thermal fluid	Ethylene glycol / deionized water
Operational mode	Isothermal for measurement of battery enthalpic and entropic changes, efficiency, lifetime and performance
Maximum battery size	12 x 8 x 6 inches
Baseline noise	5 mW
Baseline stability	30 mW
Maximum power	50 W
Maximum current	250A
Maximum voltage	50V
Enthalpy accuracy	± 2%

The instrument is semi-automated. Most of the operations are controlled manually from the front panel of LabVIEW based data acquisition system. The calorimeter can measure heat generated by any battery chemistry in the range from 100mW to 50W.

The images of the calorimeter and its chamber are shown in Fig. 2.

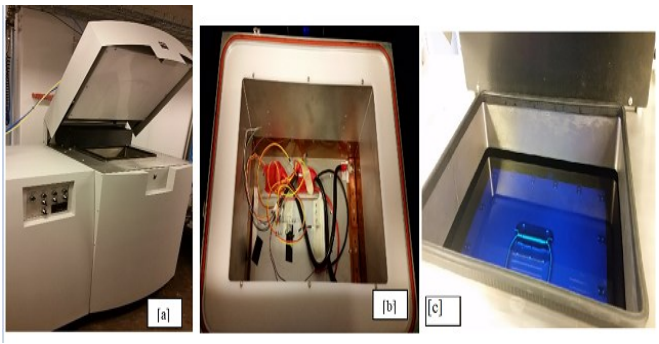

Fig. 2. Isothermal Calorimeter for measuring the thermal behavior of battery cells. (a)The external outlook of the calorimeter. (b) The internal outlook of the calorimeter chamber (c)The experimental condition: calorimeter chamber is submerged in liquid (50% ethylene glycol and 50% water solution).

It should be noted that the calorimeter has a high thermal inertia which limits its heating or cooling rates. A maximum of five Kelvin per hour can be reached. For instance, when starting from 25°C for an experiment to be run at 40°C, so it may take 3 hours to reach temperature equilibrium.

C. PTC10 Temperature Controller

Employed PTC10 Programmable Temperature Controller is manufactured by the Stanford Research System™. It is a modular system that is used for temperature control of the calorimetric experiment. So, it is configured for measuring temperature, controlling heaters, and logging temperature data of the experiments. It is connected with four I/O cards. Those are two types of input cards for Resistance Temperature Detectors (RTDs) and thermocouples, and two types of output cards for driving heaters. The PID feedback control channels are controlled by the LabVIEW-based control panel. It has 50 Hz PID sampling rate with one mK resolution.

D. Data Acquisition(DAQ) system

The corresponding experiment parameters are set up on the front panel of the LabVIEW-based GUI control program. Those include temperature set-point, PID control parameters for temperature control, DAQ sampling rate. Those are defined using the front panel of the GUI.

A DAQ chassis with 4-channel 24 bits analog input module (±10V) is used for the interface between I/O cards and communication with the computer. This DAQ system is made up of several channels. The following instruments data are acquired by the DAQ system:

a) 4-channel 24 bits PT100 RTD analog input

b) 4-channel 24 bits ±80mV thermocouple analog input

For temperature control, a proportional-integral-differential (PID) feedback loop is used. It is used to control the power supplied to a heater. It is the main driving force to keep the bath temperature in a stable limit.

E. Calibration of the calorimeter

The specific calibration is carried out using the precision resistance provided with the calorimeter instrument. It is accomplished by applying the three different Joule effect pulses. The goal of this particular calibration is to reproduce the heat flux measurement as closely as possible in comparison to the conditions of the experiment.

The Joule effect calibration is used. In this calibration, the electrical energy is dissipated by the resistance. There is an assumption that 100% of this energy is converted into heat energy. The actual heat is measured by the heat flux sensors inside the calorimeter. There is a comparison of the joule energy with sensor measured value. It provides a base for calculating a calibration coefficient for the given temperature.

Shunt resistance is used for measuring the current during charge and discharge in order to find the calibration factor. However, this calibration factor depends on the exact value of the resistance that is used in the research. In the current experimental condition, a particular resistance is used. It generates a 50mV voltage for 300A current and having a resistance value of 0.167mΩ. Calibration of the calorimeter is accomplished by applying a controlled electrical current to this accurate resistance located inside the calorimeter chamber. This type of calibration is common for most of the types of the calorimeter. The power of the different Joule effect pulses, created in the calorimeter, is adapted to the measuring range of the instrument (100mW to 50W). The calibration is also performed at many different temperatures (-30°C, 0°C, +30°C or +60°C).Fig. 3 provides a plot of the Joule effect calibration.

1) Calibration polynomial

Most of the experiments need to be run at temperatures other than -30°C, 0°C, +30°C or +60°C. In that case, to obtain a good accuracy, a calibration polynomial is used. By using the calibration polynomial for calculating the calibration coefficient at the particular temperature may lead to an additional error of measurement (less than 1%). The standard calibration is comprised of 3 successive Joule effect pulses at different levels of power 100mW, 1W, and 10W. The goal of this particular calibration would be to obtain the exact calibration coefficient for the specific temperature of the experiment. It has to be noted that the calibration points are machine specific. The calibration points are provided in TABLE II.

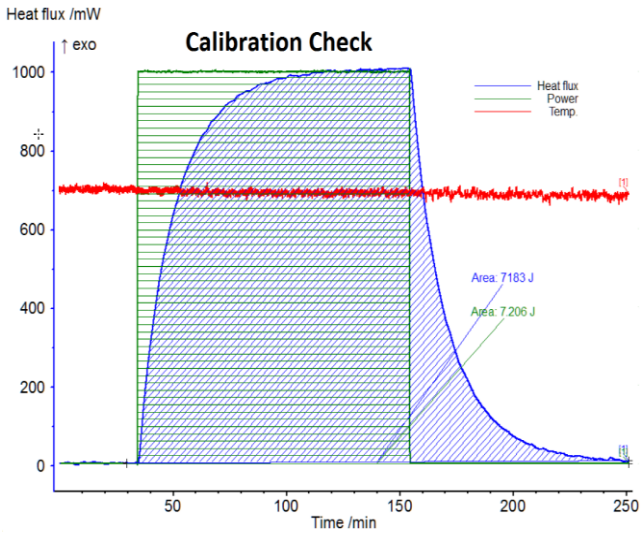

Fig. 3. Joule effect calibration graph for the calorimeter using the calibration resistor. The input power and heat flux proportion contribute to the determination of the calibration coefficient for the particular calorimeter.

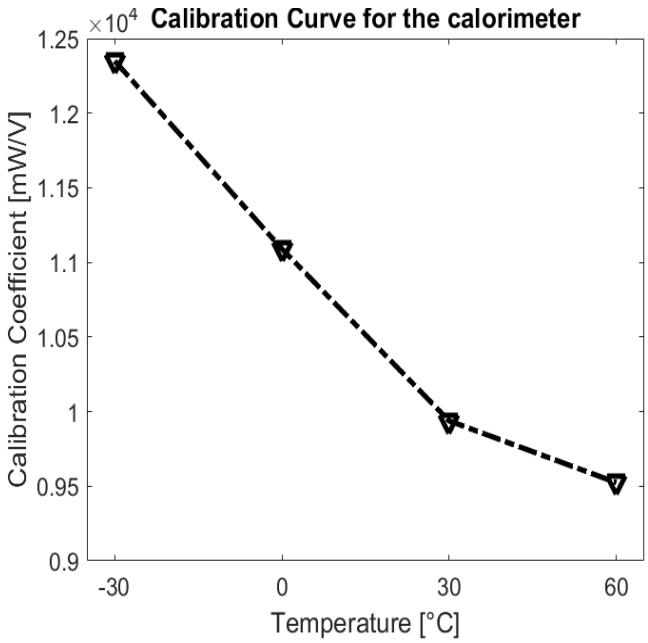

Fig. 4. Calibration curve of the calorimeter.

TABLE II. CALIBRATION COEFFICIENTS MEASURED AT DIFFERENT TEMPERATURES OF NETZSCH IBC 284 CALORIMETER. THE CALIBRATION COEFFICIENTS ARE CALORIMETER DEPENDENT.

Temperature (°C)	Calibration coefficient (mW/V)
-30	12349.71
0	11090.34
+30	9937.88
60	9524.43

From different calibration points, various calibration coefficients are calculated. Consequently, a calibration polynomial can be generated as shown in Fig. 4.

The resulting calibration polynomial equation expresses the calibration coefficient as a function of temperature. Calibration coefficient can be fitted by the third order polynomial using the data points from the calibration test (refer to Fig. 4).

$$\text{Calibration coefficient } (T) = 0.0039T^3 + 0.0594T^2 - 43.709T + 11090 \quad (1)$$

In the last step, the calibration polynomial is verified at the particular temperature and for three levels of power: 500mW, 2W, and 8W. It is ensured that the error of measurement on each pulse remains within ±2%.

F. Experimental conditioning and battery cell preparation

Nitrogen as the inert gas atmosphere is used for the calorimeter chamber. Swagelok connector is used to connect the gas connections, and it is ensured that inlet pressure of the gas is kept less than 15 psi. This gas is used for over pressurizing (up to maximum three psi) in the calorimeter chamber. Principally, this is done for safety. Due to this, the liquid cannot get into the chamber in the case of sealing failure. Clean and dry compressed air is used for the fluid level management. Inlet pressure of this is kept less than 30psi for the compressed gas as recommended by the manufacturer. Predominantly, the compressed air is used to push the liquid from a tank located on the bottom of the instrument to the bath in which the calorimeter is seated. Burst disk is set at 5 psi for safeguard the calorimeter chamber. The regular pressure in the calorimeter is controlled with a 2-point regulation (1.5 psi being the lowest limit and 3psi the highest). To achieve excellent temperature homogeneity inside the isothermal bath, constant stirring is ensured in the experimental condition.

After proper calibration, the calorimeter is ready for real life measurements on battery cell. The bath temperature set point is to be adjusted. Before this, using data acquisition software, parameters are set using the front panel of GUI. Prior to electrically connecting the battery sample inside the calorimeter, the battery cell sample needs to be prepared. This is because it can be easily attached to the existing calorimeter connections. To be tested, the battery sample needs to be equipped with two wires for powering purpose and two wires for sensing. It is schematically represented in Fig. 5.

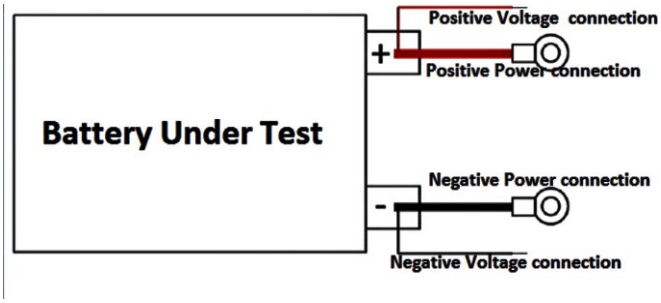

Fig. 5. Voltage and power connections of the battery while it is placed in the calorimeter's chamber.

The thermal contact between the battery sample and the calorimeter is the most important factor for obtaining the accurate data. This ensures a seamless heat transfer between the battery itself and the bottom plate of the calorimeter. It is to be noted that the thermoelectric sensors are located underneath of the battery chamber. Four contact thermocouples are put on the battery cell surface as shown in Fig. 6.

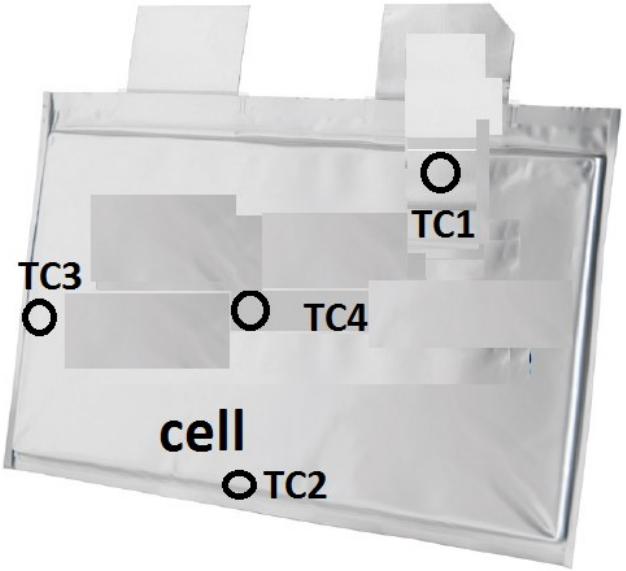

Fig. 6. Illustration of thermocouples' position on the battery cell surface. Four thermocouples are used (axial edge, lateral edge, battery tab and battery center).

Once the experiment has been set up, the calorimeter chamber lid is closed. Consequently, the calorimeter is pressurized, and the isothermal bath is filled with the calorimeter liquid, and it is kept above the lid of the calorimeter chamber (refer to Fig. 1). A continuous Stirring is ensured during the experiment. Moreover, it is ensured that calorimeter chamber pressure is higher than two psi. Bath temperature stability should be better than 0.01°C for a period of at least one hour.

IV. Results and Discussion

After performing the calibration and experimental conditioning, the battery sample is electrically connected with battery cycler. Kepco® bidirectional power supply is used as a battery cycler.1C (13A) current charging protocol is applied up to 2.8V and followed by constant voltage charging until cut-off current equal to 0.52A. On the other hand, a 13A (1C) constant current discharge is applied with a cut-off voltage equal to 1.5 V.

The experiment is carried out both at 25°C and at 0°C.There is a calibration factor that is 11090.34 mW/V determined by 0°C. But the calibration coefficient at 25°C is calculated as 10095 mW/V using Eqn. (1). After acquiring the data, Netzsch® Proteus® Software is used for the thermal analysis.

A. Heat Generation inside the cell

For the given current rate during full charging and discharging (cycling), a separate heat calculation is pursued, so the peaks (refer to Fig. 7) depict heat during battery charging and discharging respectively.

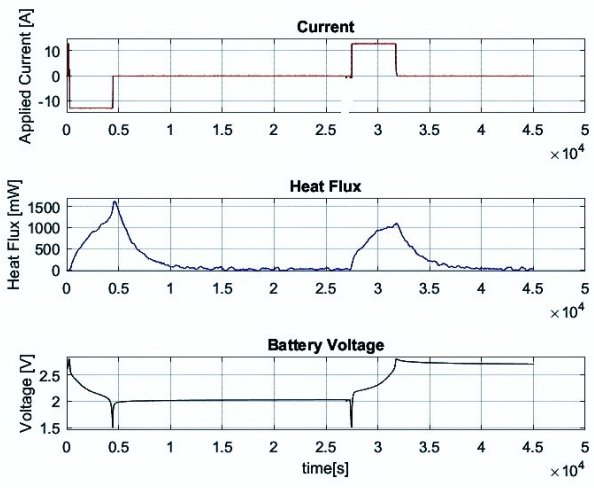

Fig. 7. Battery current, heat flux, and battery voltage in function of time.

Heat flux area represents the integration of the measuring raw heat sensor data measured by a calorimeter. To directly calculate heat flux from the raw heat flux measurement, it is needed to set up the left limit of the area, just before the required experiment (for example discharge) starts. Moreover, it is to be ensured that the heat flux background noise is within ±10mW at least for 1-hour period (refer to Fig. 8). After finishing the required experiment, it is needed to set up the right limit of the area when the heat flow signal is back to its baseline value (refer to Fig. 9).

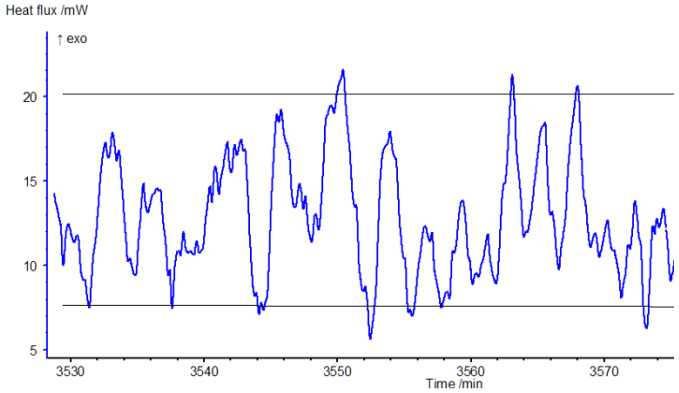

Fig. 8. Heat flux background noise. It cannot be over 20mW peak to peak at least over one hour.

It is usually necessary to correct the measuring values of the baseline for calorimetric measurements. To make a suitable baseline selection, one must be thorough and be sure to take the proper interpretation of the measured data into consideration. This is particularly important in the case when the tested battery contains not only a heat of reaction but also a change of the specific heat. To cover a multitude of possibilities in the analysis process, the appropriate baseline type is to be chosen. Baseline correction has a great influence on the parameters of inverse reaction kinetics [20]. In the current analysis, a linear baseline is used for area determination (refer to Fig. 9). The linear baseline connects the start and end values of the chosen measuring range using a straight line. As a result, all influences that are linked to a linear change of specific heat capacity (Cp) are corrected, whereas the reaction itself does not lead to a change of specific heat capacity. In the case when there is a clear indication of the thermal parameter change, (for instance: Cp), it is mandatory to choose the correct baseline type. To make a suitable baseline selection, one must be thorough and be sure to take the proper interpretation of the measured data into consideration. The mathematical description of the baseline, B(t) is given in Eqn. (2)

$$B(t) = Q(t_s) + \frac{Q(t_f)-Q(t_s)}{t_f-t_s} * (t - \mathrm{ts}) \qquad (2)$$

Where,$Q(\mathrm{t})$= Measured Calorimeter Heat Flux signal;t_s= Start time of the experiment;t_f = End time of the experiment.

After selecting the proper baseline and the range, using the computational software, the enclosed area is found (refer to Fig. 9) which represents the heat flux area.

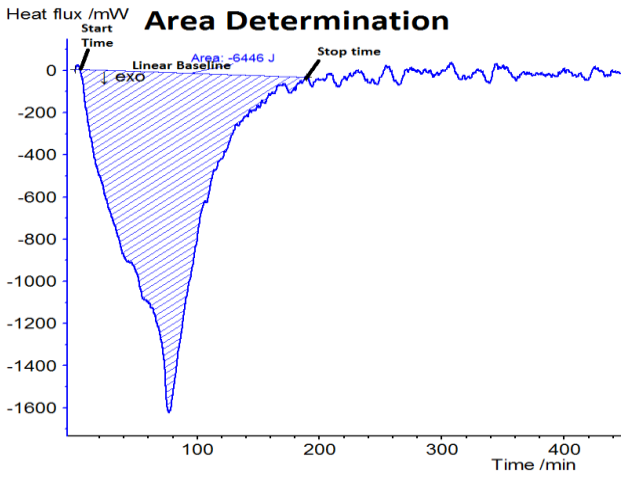

Fig. 9. The determination area of the heat flux. A suitable start and stop time are selected. The area is calculated over a linear baseline.

The amount of heat generation is determined by heat flux area divided by the of total experiment time (End time- Start time). The heat generation can be found by Eqn (3):

$$\text{Heat generation} = \frac{\text{Heat Flux}-\text{Area}}{t_f-t_s} \qquad (3)$$

B. Determination of battery efficiency

The next step is to measure battery efficiency. It is performed by determining the absolute power area. Heat flux area is subtracted from the absolute power area and normalized by the absolute power area to find the battery efficiency. Eqn. (4) is used for determining the efficiency:

$$\eta = \frac{\text{Absolute Power Area}-\text{Heat Flux Area}}{\text{Absolute Power Area}} \qquad (4)$$

The analysis of the data is accomplished using the software as shown in Fig. 10.

The summary of analysis is tabulated in TABLE III. From the calorimetric analysis, the variation of heat generation, total energy loss, efficiency and maximum temperature increase between full charging and discharging (cycling) at 25°C to cycling at 0°C is found. The analysis shows, there is a significant (164%) rise in heat generation in low-temperature discharge. In contrast, there is a moderate (approx. 33%) heat generation increase in case of battery charge for the same condition. However, total energy loss in the battery shows slight different behavior. In this case, it is observed that there exist a substantial (131.45%) increase in case of discharge total energy loss at low temperature same as the previous case.

But, the charging energy loss shows now substantial (125.88%) increase.

In the case of efficiency, there is a moderate (6.24%) gain in efficiency in case of higher temperature discharge phenomenon. Accordingly, there is a modest (3.65%) gain in charging efficiency for the same case.

The temperature of the battery cell surface is shown in the Fig. 11. To determine the maximal temperature increase, four thermocouple data are plotted as shown in Fig. 6. The maximal temperature increase corresponds the maximum temperature difference between maximum and minimum temperature among the thermocouples. It displays the amount of thermal gradient on the corresponding current rate.

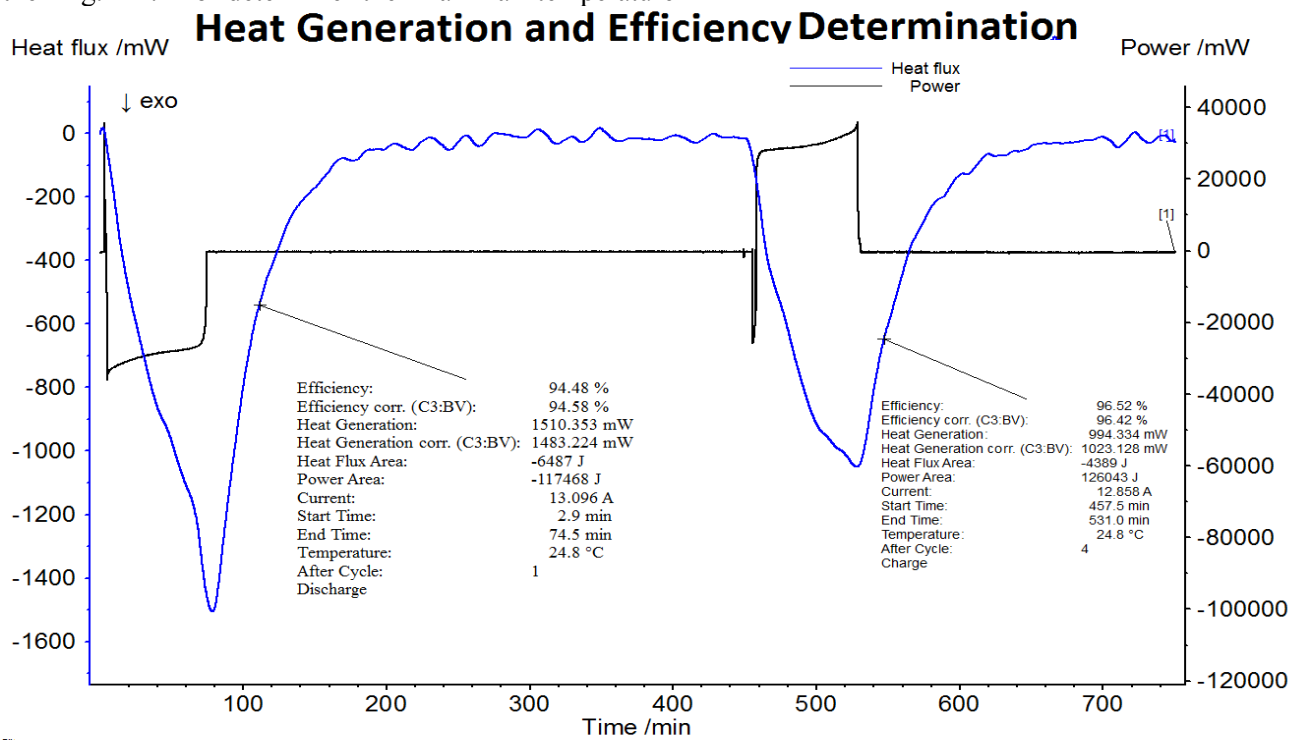

Fig. 10. A complete analysis of LTO battery cell heat generation using isothermal calorimeter.The LTO battery cell is charged following a constant current-constant voltage (CC-CV) profile and discharged using a constant current (CC) profile.

TABLE III. THE COMPLETE CALORIMETRIC ANALYSIS AT DIFFERENT TEMPERATURES AND DIFFERENT OPERATING CONDITIONS.

Attribute	Test at 0°C					Test at 25°C			
	Discharge	Charge	Discharge	Charge		Discharge	Charge	Discharge	Charge
Heat Generation (mW)	3961.415	1423.189	4005.315	1489.725		1498.498	1069.493	1521.143	1071.65
Total energy Loss (J)	14898.213	10664.569	14810.35	11201.158		6437	4721	6501	4734
Efficiency (%)	88.71	92.85	88.59	92.48		94.25	96.25	94.5	96.01
Maximum temperature increase (°C)	Not reported		Not reported			2.3	2.1	1.9	1.8

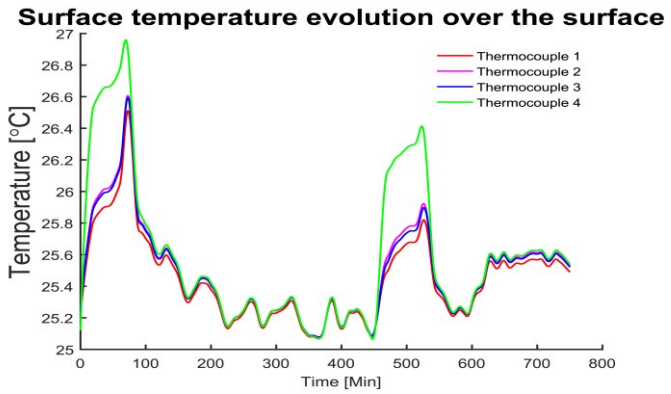

Fig. 11. Surface temperature evolution of the battery cell during 1C charging and discharge cycle. Surface temperature is measured at different points by using contact thermocouples.

V. CONCLUSION

The calorimetric experiments are used to determine efficiency and heat generation for the battery cell. Both of them are critical performance indicators for the battery operation. Evidently, the magnitude of heat generation is associated with the corresponding current rate. Particularly this fact assists on the thermal modeling. For this reason, the corresponding heat generation in function of battery current rate can be used as input as the heat source of a model. This can be conveniently accomplished by a lookup table of heat rate versus applied current profile. Furthermore, the surface temperatures that are measured in this research work can be used for the validation of the thermal model of the battery. Additionally, large cells can be tested safely and efficiently with the electro-thermal testing platform as established in the paper. The experimental platform has an enormous impact on the profiling of a battery cell. Using this established methodology, the extensive full profile of a battery cell for instance: efficiency, heat generation at different current rates and temperatures in the diverse operating condition of charge and discharge can be found.

ACKNOWLEDGMENT

The authors gratefully acknowledge the financial support for this work from the Danish Strategic Research Council to the Advanced Lifetime Predictions of Battery Energy Storage (ALPBES) project. They also acknowledge the support of R&D Director Jean-Francois Mauger of NETZSCH® Instruments North America, LLC.

REFERENCES

[1] G. H. Kim, K. Smith, K. J. Lee, S. Santhanagopalan, and A. Pesaran, "Multi-Domain Modeling of Lithium-Ion Batteries Encompassing Multi-Physics in Varied Length Scales," *Journal of the Electrochemical Society,* vol. 158, pp. A955-A969, 2011.

[2] A. A. Pesaran, "Battery thermal models for hybrid vehicle simulations," *Journal of Power Sources,* vol. 110, pp. 377-382, Aug 2002.

[3] M. R. Khan, M. P. Nielsen, and S. K. Kær, "Feasibility Study and Techno-economic Optimization Model for Battery Thermal Management System," in *Proceedings of the 55th Conference on Simulation and Modelling (SIMS 55), Modelling, Simulation and Optimization*, Aalborg,Denmark, 2014, pp. 16-27.

[4] M. R. Khan, G. Mulder, J. Van Mierlo, and S. K. Kær, "The Integration and Control of Multifunctional Stationary PV-Battery Systems in Smart Distribution Grid," in *EU PVSEC The 28th European Photovoltaic Solar Energy Conference and Exhibition* Paris, France, 2013, pp. 3841 - 3851.

[5] J. Newman, K. E. Thomas, H. Hafezi, and D. R. Wheeler, "Modeling of lithium-ion batteries," *Journal of Power Sources,* vol. 119, pp. 838-843, Jun 2003.

[6] M. R. Khan, S. J. Andreasen, and S. K. Kær. (2014, 01.08.2014) Novel Battery Thermal Management System for Greater Lifetime Ratifying Current Quality and Safety Standard. *Battery Connections*. 6-10.

[7] T. M. Bandhauer, S. Garimella, and T. F. Fuller, "A Critical Review of Thermal Issues in Lithium-Ion Batteries," *Journal of the Electrochemical Society,* vol. 158, pp. R1-R25, 2011.

[8] M. R. Khan, J. V. Barreras, A. I. Stan, M. Swierczynski, S. J. Andreasen, and S. K. Kær, "Behavior Patterns, Origin of Problems and Solutions Regarding Hysteresis Phenomena in Complex Battery Systems," in *Hysteresis: Types, Applications and Behavior Patterns in Complex Systems*, J. C. Dias, Ed., First ed: Nova Science Publishers 2014, pp. 215-226.

[9] M. R. Khan, G. Mulder, and J. Van Mierlo, "An online framework for state of charge determination of battery systems using combined system identification approach," *Journal of Power Sources,* vol. 246, pp. 629-641, 1/15/ 2014.

[10] G. Vertiz, M. Oyarbide, H. Macicior, O. Miguel, I. Cantero, P. Fernandez de Arroiabe, *et al.*, "Thermal characterization of large size lithium-ion pouch cell based on 1d electro-thermal model," *Journal of Power Sources,* vol. 272, pp. 476-484, 12/25/ 2014.

[11] J. Vetter, P. Novák, M. R. Wagner, C. Veit, K. C. Möller, J. O. Besenhard, *et al.*, "Ageing mechanisms in lithium-ion batteries," *Journal of Power Sources,* vol. 147, pp. 269-281, 9/9/ 2005.

[12] H. G. Sun, X. H. Wang, B. Tossan, and R. Dixon, "Three-dimensional thermal modeling of a lithium-ion battery pack," *Journal of Power Sources,* vol. 206, pp. 349-356, May 2012.

[13] D. Brown and R. G. Landers, "Control Oriented Thermal Modeling of Lithium Ion Batteries from a First Principle Model via Model Reduction by the Global Arnoldi Algorithm," *Journal of the Electrochemical Society,* vol. 159, pp. A2043-A2052, 2012.

[14] R. Kizilel, R. Sabbah, J. R. Selman, and S. Al-Hallaj, "An alternative cooling system to enhance the safety of Li-ion battery packs," *Journal of Power Sources,* vol. 194, pp. 1105-1112, Dec 2009.

[15] M. R. Khan and S. K. Kær, "Multiphysics Based Thermal Modeling of a Pouch Lithium-Ion Battery Cell for the Development of Pack Level Thermal Management System," in *EVER 2016 (Eleventh International Conference on Ecological Vehicles and Renewable Energies)* Grimaldi Forum, Monaco, 2016.

[16] M. R. Khan and S. K. Kær, "Modeling Thermal Effects of Battery Cells Inside Electric Vehicle Battery Packs," in *2015 COMSOL Conference*, Grenoble, France, 2015.

[17] K. Somasundaram, E. Birgersson, and A. S. Mujumdar, "Thermal–electrochemical model for passive thermal management of a spiral-wound lithium-ion battery," *Journal of Power Sources,* vol. 203, pp. 84-96, 4/1/ 2012.

[18] Z. H. Rao and S. F. Wang, "A review of power battery thermal energy management," *Renewable & Sustainable Energy Reviews,* vol. 15, pp. 4554-4571, Dec 2011.

[19] K. Smith, G.-H. Kim, E. Darcy, and A. Pesaran, "Thermal/electrical modeling for abuse-tolerant design of lithium ion modules," *International Journal of Energy Research,* vol. 34, pp. 204-215, 2010.

[20] ISO, "ISO 11357-1:2009 Plastics -- Differential scanning calorimetry (DSC) -- Part 1: General principles," ed: ISO, 2009.